Nanoscale

Dynamic Article Links

Cite this: *Nanoscale*, 2011, **3**, 4989

www.rsc.org/nanoscale

PAPER

Mechanism and determinants of nanoparticle penetration through human skin

Hagar I. Labouta,[ab] Labiba K. El-Khordagui,[b] Tobias Kraus[c] and Marc Schneider*[a]

Received 15th August 2011, Accepted 4th October 2011
DOI: 10.1039/c1nr11109d

The ability of nanoparticles to penetrate the stratum corneum was the focus of several studies. Yet, there are controversial issues available for particle penetration due to different experimental setups. Meanwhile, there is little known about the mechanism and determinants of their penetration. In this paper the penetration of four model gold nanoparticles of diameter 6 and 15 nm, differing in surface polarity and the nature of the vehicle, through human skin was studied using multiphoton microscopy. This is in an attempt to profoundly investigate the parameters governing particle penetration through human skin. Our results imply that nanoparticles at this size range permeate the stratum corneum in a similar manner to drug molecules, mainly through the intercellular pathways. However, due to their particulate nature, permeation is also dependent on the complex microstructure of the stratum corneum with its tortuous aqueous and lipidic channels, as shown from our experiments performed using skin of different grades of barrier integrity. The vehicle (toluene-*versus*-water) had a minimal effect on skin penetration of gold nanoparticles. Other considerations in setting up a penetration experiment for nanoparticles were also studied. The results obtained are important for designing a new transdermal carrier and for a basic understanding of skin–nanoparticle interaction.

Introduction

The potential ability of nanoparticles to overcome the barrier function of the stratum corneum (SC) has been recently the target of several studies. Nevertheless, there is a controversy among researchers whether nanoparticles do penetrate the SC into the viable tissue[1,2] or not.[3–5] The different results are mainly due to different experimental setups in terms of the skin type, skin surface area, exposure time and type and concentration of applied nanoparticles. A great deal of the recent work was mainly focused on treating the skin physically, *e.g.*, tape stripping,[6,7] mechanical flexion,[8] UV exposure,[9] sonophoresis,[10] microneedles[11] or chemically using penetration enhancers[12] to cause or enhance the penetration of nanoparticles into the deeper skin layers (DSL). In this study, however, a well-designed skin penetration experiment, using excised human skin as the gold standard for *ex vivo* skin penetration is considered crucial in regard to the extensive studies on animal skin.[1,7,8,13,14] The physicochemical parameters, size, surface polarity, physical state of the nanoparticles, in addition to the effect of vehicle were in focus.

The surface polarity of the nanoparticles and the nature of the vehicle are expected to play a role in skin-penetration of nanoparticles. Yet, to our knowledge, only three studies investigated the effect of surface charge of nanoparticles on skin penetration, though they were also controversial in terms of the surface charge which leads to higher affinity of the particles to porcine skin.[1,15,16] Senzui *et al.*[17] studied the penetration of 35 nm titanium dioxide nanoparticles, uncoated and coated with alumina/silica/silicon, through porcine skin. However, no penetration was reported for both particles.

Apart from the size factor, the effect of the surface polarity of nanoparticles with the same diameter on skin penetration has not been the scope of any investigation so far. On the other hand, the only evidence for the effect of solvents on the skin penetration of nanomaterials was recently reported by Xia *et al.*[13] for pristine fullerenes of 1 nm in diameter. Several industrial organic solvents: chloroform, toluene, cyclohexane and mineral oil were examined. Porcine skin biopsies showed penetration of particles for all of the tested solvents except for mineral oil, with much higher penetration in case of chloroform. Baroli *et al.*,[18] however, compared the effect of nanoparticle formulation to blank solutions on human skin resistivity and concluded a minor effect of the vehicle on their results. Finally, the physical stability of nanoparticles when coming in contact with the skin and its effect on skin penetration, though not studied so far, is an important parameter that could partly explain the disagreement of results reported by different researchers concerning the penetration of nanoparticles of the same size range.[1,4] Hence, a more systematic study on the penetration of nanoparticles through human skin

[a]*Pharmaceutical Nanotechnology, Saarland University, 66123 Saarbrücken, Germany. E-mail: marc.schneider@mx.uni-saarland.de; Fax: +0049 681 302 4677; Tel: +0049 681 302 2438*
[b]*Department of Pharmaceutics, University of Alexandria, 21521 Alexandria, Egypt*
[c]*Structure Formation Group, Leibniz Institute for New Materials (INM), 66123 Saarbrücken, Germany*

taking into account all the mentioned relevant physicochemical parameters together has not been done so far.

Several nanoparticles, polymeric or inorganic nanoparticles, were investigated for possible skin penetration.[19] Among these particles, gold nanoparticles (AuNP) are considered a good model for studying skin penetration of nanoparticles.[20–22] They have unique optical properties. They show distinctive extinction bands in the visible region, due to surface plasmon oscillation of free electrons.[23] This property allows for tracking the physical state of the particles under different conditions throughout the experiment and for their detection in human skin. AuNP have also high clinical significance due to their ability to deliver various payloads[24–26] such as drug molecules,[27] large biomolecules, such as proteins,[28] DNA,[29,30] or RNA.[31] Moreover, AuNP cause local heating when they are irradiated with light in the visible range allowing for the potential use of AuNP in photothermal destruction of tumors.[32]

In an earlier study, we reported on the consequences of topical exposure to two selected polar and apolar gold nanoparticles in regard to their effect on skin metabolism and penetration into deeper layers of human skin using multiphoton tomography and fluorescence lifetime imaging.[33] The present work, however, is a mechanistic study of the penetration of nanoparticles into human skin using a full matrix of particles of different surface polarity, size and vehicle. In addition, the concentration of applied nanoparticles, skin exposure time, the physical state of the particles on skin exposure and skin integrity were investigated.

Materials and methods

Preparation of apolar gold nanoparticles in toluene (AuNP1)

Sterically stabilized, apolar gold nanoparticles (AuNP1) were synthesized from an organometallic precursor. The synthetic procedure was adapted from Zheng *et al.*[34] Gold nanoparticles were formed upon reduction of the gold source by an amine–borane complex in the presence of an alkyl thiol. In a typical synthesis, 0.31 g chlorotriphenylphosphine gold (purity 98%, ABCR, Karlsruhe, Germany) was dissolved in 50 ml of benzene (purity >99.5%, Riedel-de Haen, Germany) forming a colorless solution. A mixture of 0.53 g *tert*-butylamineborane (purity, 97%, Fluka, Germany) and 0.31 ml dodecanethiol (purity >98%, Fluka, Germany) were added to the formed solution and left to react at 55 °C for 1 h. Upon completion of the reduction reaction, the red solution was cooled to room temperature, precipitated by the addition of ethanol and washed by centrifugation and subsequent resuspension in toluene. Finally, the particles were resuspended in toluene and stored at room temperature protected from light.

Phase transfer of apolar AuNP1 into water. AuNP1 were transferred into water using an emulsification method. A solution of 10 g lecithin (pure lecithin (98% phospholipids), Boma-Lecithin GmbH, Otter, Germany) in 400 ml water was prepared and stirred overnight to ensure complete dissolution. About 40 ml of the AuNP dispersion in toluene was added to the solution and the mixture was shaken and further emulsified at the maximum energy of an ultrasonic bath (Elmasonic S100H, Elma GmbH & Co KG, Singen, Germany) for 5 min and at half its maximum energy for 15 min, followed by heating it to 90 °C under stirring for 1 h. This procedure was repeated several times to ensure emulsification and toluene evaporation. Unemulsified parts of the AuNP dispersion were separated from the mixture and emulsified separately using additional sonication steps. Finally, AuNP2 dispersion with hydrophilized surface was stirred at 90 °C until all toluene had evaporated leaving a clear red aqueous solution.

Preparation of polar gold nanoparticles in toluene (AuNP3)

Ionically-stabilized, polar gold nanoparticles (AuNP3) were prepared according to Turkevich method.[35] Briefly, 70 ml solution of hydrogen tetrachloroaurate ($HAuCl_4 \cdot 3\ H_2O$, Sigma-Aldrich Chemie GmbH, Steinheim, Germany) containing about 100 μg ml^{-1} gold was first heated to boiling at 100 °C under magnetic stirring at about 440 rpm and then reduced by a solution of trisodium citrate dihydrate ($Na_3C_6H_5O_7 \cdot 2H_2O$, Sigma-Aldrich) containing 5-fold the molar concentration of the gold salt. All solutions were used without filtration. After the gold colloid had formed, the temperature was lowered to about 25 °C. The colloid was then transferred into a suitable glass container and stored in the refrigerator protected from light.

Phase transfer of polar AuNP3 into toluene. The method of phase transfer followed the protocol published by Zhu *et al.*[36] after several modifications. Practically, a volume of thioglycolic acid (TGA) ($C_2H_4O_2S$, 99%, Sigma-Aldrich Chemie GmbH, Steinheim, Germany) equivalent to 1.29×10^{-3} moles was added to 2 ml of an AuNP dispersion, with a concentration of 99.05 μg ml^{-1} gold and stirred until the solution gets purple, indicating chemical bonding of –SH group of TGA onto the surface of AuNP. *N*-Cetyl-*N*,*N*,*N*-trimethylammonium bromide (cetrimide) ($C_{19}H_{42}BrN$, Merck KGaA, Darmstadt, Germany) was then introduced to the AuNP dispersion portionwise while stirring. The molar ratio between TGA and cetrimide is 2 : 1. Stirring was continued for 30 min to allow for the adsorption of surfactant molecules through electrostatic interaction between TGA and cetrimide. A volume of 2 ml toluene was then mixed with the dispersion for 10 min, resulting in O/W emulsion. Finally, 2 ml ethanol, containing 0.21 M cetrimide, was added to break the emulsion, in addition to 3 ml toluene for better extraction of AuNP with hydrophobized surface. The whole two-phase system was vigorously shaken for 20 min. Ethanol is miscible with water, thus the dissolved cetrimide further coat AuNP that are still in the aqueous phase resulting in more particles transferred into toluene. Extracted AuNP in toluene were further treated with cetrimide. A weight of cetrimide equivalent to 6.86×10^{-6} moles is required for each 1 ml of prepared AuNP4 dispersion to keep it stable over a prolonged period of time.

Characterization of the optical and colloidal properties for the prepared AuNP

The optical properties of prepared AuNP were checked using a UV/Vis Spectrophotometer (lambda 35, Perkin Elmer, Rodgau-Jürgesheim, Germany) in the range of 400–800 nm. The

mean particle size and the morphology of the gold core were determined by transmission electron microscopy (TEM) using a JOEL Model JEM 2010 instrument (JOEL GmbH, Eching, Germany) operated at an accelerating voltage of 120 kV. Core diameters determined by TEM were used as particle size facilitating comparison of particle diameters as hydrodynamic radius is only available in aqueous solution. Samples for TEM analysis were prepared by placing 12 μl drop of dispersed nanoparticles in water on carbon-coated 400 mesh copper grid. The solvent was allowed to evaporate slowly at room temperature. Finally, the surface charge of AuNP2 and AuNP3 was estimated by measuring the zeta potential based on the electrophoretic mobility (Zetasizer Nano, Malvern Instruments, Malvern, UK). The prepared dispersions (1.5 ml) were directly measured (solvent is water) in triplicate using disposable folded capillary cells that contained the electrodes. Measurements were done at room temperature. Since particle dispersion in the non-polar solvent, toluene, in case of AuNP1 and AuNP4, would not allow for development of surface charge (though a value near zero could be measured by zetasizer), this was denoted as "uncharged" in Table 1.

Study of the penetration of AuNP through human skin

Skin preparation. Human skin obtained from female patients aged 30 to 57 years, who had undergone abdominal plastic surgery was used for skin experiments after approval of the ethic committee of Saarland, Germany (Ärztekammer des Saarlandes, Dec. 2008); three skin donors were used in the study. Adequate health and no medical history of dermatological disease were required. Immediately after excision, the skin was cut into pieces and the subcutaneous fatty tissue was removed from the skin specimen using a scalpel. Afterwards the surface of each specimen was cleaned with water, wrapped in aluminum foil and stored in polyethylene bags at −26 °C until used. Previous investigations have shown that no change in the penetration characteristics occurs during the storage time of 6 months.[37]

Skin discs, 25 mm in diameter, were punched out from frozen skin, thawed, cleaned with deionized water and transferred into the Franz diffusion model.

Skin penetration study. *In vitro* penetration experiments were run in static Franz diffusion cells having a diffusion area of 1.76 cm^2 and a receptor compartment of 12 ml volume. The prepared human skin was fastened carefully between the donor and receptor compartments, with the SC side up and held in place with a clamp. The dermal side of the chamber contained a receptor solution of phosphate buffer saline, pH 7.4 magnetically stirred at 500 rpm. A volume of 500 μl of the prepared AuNP dispersion was placed on the skin then the donor compartment was occluded. The diffusion cells were maintained at 32 °C throughout the experiment. Following exposure, the skin was removed and the skin surface was gently cleaned with cotton. Collected skin was examined after longitudinal cryo-sectioning and the donor solution was analyzed directly by UV/Vis spectroscopy to determine the physical state of the particles following skin contact.

Additional penetration experiments involved skin pre-exposure to toluene (vehicle) or chloroform–methanol mixture (discussed later) or tape-stripping of the stratum corneum before application of particle dispersion. Infrared densitometry was used for determining the endpoint of tape-stripping, *i.e.* complete SC removal, a method described by Hahn *et al.*[38]

Longitudinal skin cryo-sectioning. Cross-sections of ~10 μm thickness were performed at −20 °C using a Frigocut 2800 cryostat (Reichert-Jung, Leica, Wetzlar, Germany). It is important to note here that on sectioning, the skin piece should not be placed tangential to the blade to avoid dislocation of the particles from outside into DSL or *vice versa*, but in a perpendicular direction to the cutting blade limiting sectioning artifacts. Skin sections were placed on microscopical slides and were stored at −20 °C until imaged by multiphoton laser scanning microscopy. Before examination, specimens were mounted by an aqueous mounting medium (FluorSave™ reagent, Calbiochem, San Diego, USA) and covered with glass cover slips. At least 20 cuts were used for microscopic examination.

Multiphoton laser scanning microscopy. Fluorescence imaging was performed using an inverted confocal/two photon excitation fluorescence microscope (ZEISS LSM 510 META, Carl Zeiss, Jena, Germany), equipped with a tunable pulsed IR laser (λ = 705–980 nm) (Chameleon, Coherent, Dieburg, Germany) for multiphoton laser microscopy, in addition to other conventional laser lines for confocal microscopy. The objective used was a water immersion lens 63× (NA = 1.2). A wavelength of 800 nm was used for both excitation of AuNP and scanning the skin using a transmission energy of 0.485 and 0.647 mW in the focal plane, respectively. The optical settings, discussed in detail earlier,[33] allowed for the separation of both signals with no signal interference among tracks. z-Stacks of the skin samples were taken with steps every 1 μm. Each optical scan is composed of 512 × 512 $pixels^2$ and a size of 0.14 x 0.14 μm^2. The gain settings were adjusted for each measurement individually. No significant photobleaching has been observed in our experiments under the conditions used to quantify penetration.

Table 1 Characteristics of the prepared AuNP dispersions

AuNP code	Surface chemistry	Diameter of gold core[a]/nm	Zeta potential[b]/mV	Vehicle
AuNP1	Dodecanethiol	6.00 ± 0.81	Uncharged	Toluene
AuNP2	Lecithin	6.00 ± 0.81	−53.5 ± 1.44	Water
AuNP3	Citrate ions	14.90 ± 1.76	−35.1 ± 1.87	Water
AuNP4	Cetrimide	14.90 ± 1.76	Uncharged	Toluene

[a] measured by TEM (n is more than 30). [b] given as a criterion indicating surface charge.

Data analysis. Multiphoton images of the longitudinal skin sections were then analyzed using the software by the supplier. Semiquantitative data for the distribution of AuNP in different skin layers were extracted as published earlier. Shortly, z-stacks were adopted for analysis. For each optical layer, the intensity was first thresholded in order to remove the background. Pixels due to the luminescence of AuNP were determined in the SC and in the DSL for this optical layer. Summing up these values in all the optical layers of the z-stack ends up with $\sum$pixel frequency due to AuNP in the SC and in DSL of this z-stack, from which the weighed number of particles N_W were calculated according to eqn (1)

$$N_w = \frac{\sum \text{Pixel} \times A_{\text{pixel}}}{A_{\text{particle}}} \quad (1)$$

where $A_{\text{pixel}} = 0.139 \times 0.139$ μm^2 and A_{particle} (area of diffraction-limited AuNP) = ~0.365 μm^2 for the optical settings used in this study as detailed elsewhere.[20] It should be noted here that the summed value developed by data analysis is regarded as a semi-quantitative index to compare penetration into the SC and DSL under the same conditions as well as for different formulations and conditions.[20]. Summed values were found more informative than mean values (±SD) due to the non-homogeneous distribution of the particles throughout the diffusion area. In other words, a summed value on analysis of x number of image fields offers a relatively more rigid and resistant parameter to the great variability of particle localization.

Finally, maximum penetration depths could be also determined for these skin experiments.

Study of the vehicle effect on skin penetration of AuNP

Gravimetric analysis

Preparation of epidermal sheets. Heat-separated human epidermal sheets were prepared from specimens of full thickness human skin of 15 or 25 mm diameter according to Kligman and Christophers.[39] Shortly, full thickness human skin was immersed in water of 60 °C for 90 s. The epidermis was then carefully peeled off the dermis using forceps.

Determination of the wet and dry weights of the epidermis. Heat-separated epidermal sheets are then carefully dried using a filter paper and weighed on Teflon sheets. This represents the wet weight of the epidermis. Epidermal sheets were then dried for two days in a dessicator at room temperature then weighed once more to obtain the dry weight of the epidermis.

Determination of lipid amount extracted by toluene. Epidermal sheets, prepared from 25 mm skin punches, were fitted in static vertical Franz diffusion cells having a diffusion area of 1.76 cm^2 and a receptor compartment of 12 ml volume. The receptor compartment was filled with phosphate buffer saline, pH 7.4 and magnetically stirred at 500 rpm. A volume of 500 μl toluene was used as a donor solution for 0.5, 2, 6 and 24 h and the donor compartment was occluded. At the end of the skin exposure time, the donor solution was filtered and dried under nitrogen. Dried lipid extracted by the donor solution was then placed in a dessicator overnight and weighed for the lipid amount.

Determination of the total epidermal lipid content. Another set of epidermal sheets, prepared from 15 mm skin punches, were used to determine the total amount of lipid present in the epidermis of this skin donor having the same diffusion area as in Franz diffusion experiment. Each epidermal sheet was extracted with 5 ml chloroform–methanol, 2 : 1 in well-closed test tubes for 24 h under mild shaking. As described above, solutions were filtered, dried and lipid amounts were weighed.

High performance thin layer chromatography (HPTLC)

Dried lipid extracts of 2 h skin exposure were then redispersed in 100 μl toluene or chloroform–methanol, 2 : 1 and a volume of 1–5 μl of the lipid extract was spotted on silica gel 60-HPTLC plates (Merck KGaA, Darmstadt, Germany) along with 1 μl spots of standard solutions containing serial concentrations of cholesterol, cholesteryl oleate, glyceryl trioleate, oleic acid and ceramide NP (a ceramide consisting of a nonhydroxy *N*-acyl fatty acid and phytosphingosine). A maximum of 8 spots are applied on each plate of 20 × 10 cm dimensions. Plates are then separated into two groups according to the developing system. The first group was developed using the following sequential development system: (1) n-hexane–diethyl ether–acetic acid (80 : 20 : 10) for a distance of 12 cm from the spotting level; (2) n-hexane for 14 cm distance, for separation of cholesterol, oleic acid, triglycerides and cholesteryl ester. The plates were allowed to dry before the second development step. The second group of plates were developed using chloroform: methanol–acetic acid (95 : 4.5 : 0.5) for separation of skin ceramides. All plates were then dried and sprayed with a solution 10% $CuSO_4$ in 8.5% H_3PO_4 under nitrogen flow. The plates were then placed on a thermoplate at a preadjusted temperature of 110 °C and heated until 160 °C. Separated lipid fractions were then quantified using IR densitometry using Image J (version 1.43, available as freeware from http://rsbweb.nih.gov/ij/). The area under the curve was calculated for all the separated spots and quantification was based on the known quantities of the co-migrated standards used to develop a calibration curve.

Results and discussion

Monodisperse gold nanoparticles, AuNP1 and AuNP3, with ~6 and 15 nm core diameter, respectively, were successfully prepared. AuNP1 were uncharged, thiol coated and dispersed in toluene. On the contrary, AuNP3 were negatively charged due to stabilization with citrate ions and dispersed in water. In order to study the effect of surface polarity and the nature of the vehicle, in addition to size of nanoparticles on skin penetration, each of the prepared AuNP1 and AuNP3 were transferred into water and toluene, respectively, using a suitable phase transfer agent, as indicated in the Experimental section. The surface chemistry was therefore changed accordingly, keeping the core size unchanged hence having approximately same-sized particles of different surface polarity and different vehicle stability. All AuNP were fully characterized. The characteristics of the prepared AuNP are summarized in Table 1 and their TEM images are shown in Fig. 1.

The prepared and characterized AuNP were then applied to excised human skin at different concentrations and skin exposure

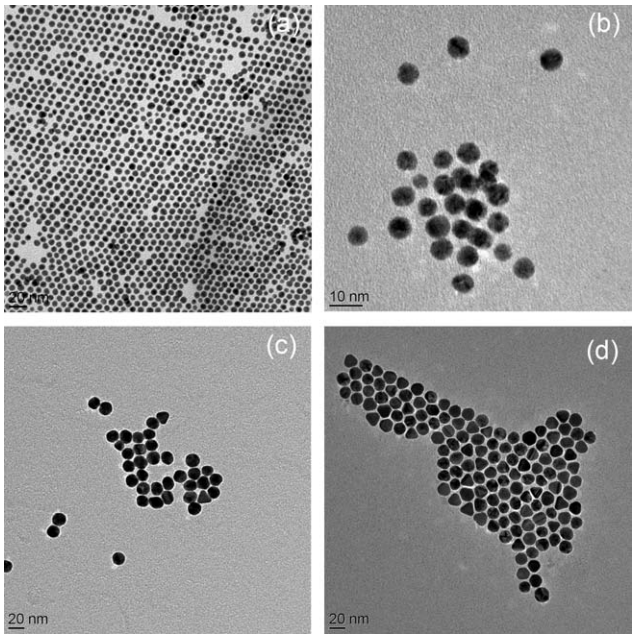

Fig. 1 TEM images of prepared (a) AuNP1 (6 nm thiol-coated AuNP, dispersed in toluene), (b) AuNP2 (6 nm lecithin-coated AuNP, dispersed in water), (c) AuNP3 (15 nm citrate-stabilized AuNP, dispersed in water) and (d) AuNP4 (15 nm cetrimide-coated AuNP, dispersed in toluene).

Table 2 Conditions of skin penetration experiments for the prepared AuNP dispersions

AuNP code	Concentration/μg ml^{-1}	Time of skin exposure/h
AuNP1	90	0.5, 2, 6 and 24
AuNP1	437	0.5, 2, 6 and 24
AuNP2	90	24
AuNP3	90	24
AuNP4	90	24

times (Table 2). After skin penetration experiment, skin punches were longitudinally sectioned and analyzed using multiphoton microscopy (Fig. 2), an efficient technique to track the penetration of nanoparticles in skin.[3,12,20,33,40] All AuNP formulations could penetrate the SC into the DSL after 24 h of skin exposure, except for AuNP3. It should be noted here that though penetration of AuNP was observed not being homogenous throughout the examined longitudinal sections, conclusion were made based on repetitive observation as indicated in the methodology section. Representative optical z-stacks, 1 μm nominal step width, for all examined longitudinal skin sections were then quantified by calculation of signal pixel frequency due to AuNP in the stratum corneum (SC) and deeper skin layers (DSL) for each optical layer. Finally a summed value of pixels ($\sum$pixel) due to AuNP in each the SC and DSL was calculated. From this parameter the weighed number of particles was calculated.[20] Therefore this method takes into account the non-homogeneous distribution of AuNP all over the diffusion area and is not dependent on one image field only. The results showed depth-profiles for AuNP with higher values in the upper skin layer, SC, decreasing reaching DSL (Fig. 3). The following factors were found to be critical in skin penetration of nanoparticles.

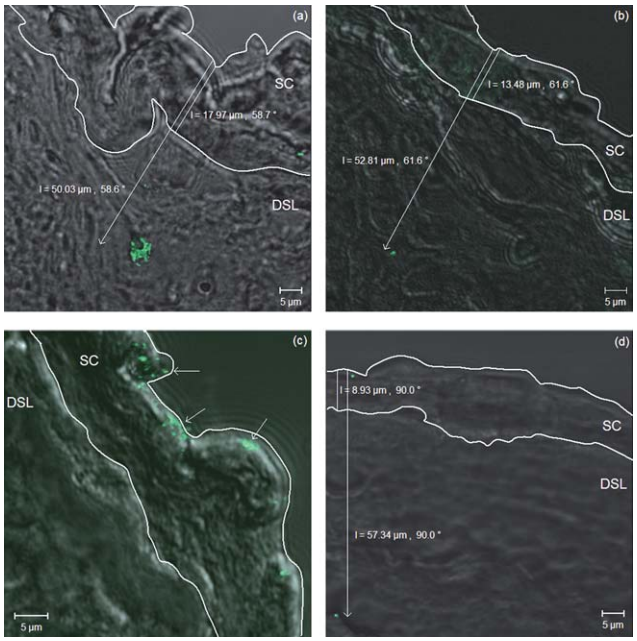

Fig. 2 Selected overlaid multiphoton/transmission images of AuNP (indicated as green pseudo-colored spots) in longitudinal skin sections in which the stratum corneum (SC) is outlined by a white line to separate it from the deeper skin layers (DSL). Skin sections were obtained from skin punches exposed for 24 h to (a) AuNP1 (6 nm thiol-coated AuNP, dispersed in toluene), (b) AuNP2 (6 nm lecithin-coated AuNP, dispersed in water), (c), AuNP3 (15 nm citrate-stabilized AuNP, dispersed in water) and (d) AuNP4 (15 nm cetrimide-coated AuNP, dispersed in toluene). As indicated in the Figure, exclusive localization of nanoparticles in the SC for AuNP3 and penetration of AuNP1, AuNP2 and AuNP4 into the DSL at variable penetration depths were observed.

Effect of size and surface polarity of AuNP

The physicochemical attributes of nanoparticles are key factors governing their skin penetration and permeation. Overlaid multiphoton/transmission microscopy images of longitudinal sections from skin specimens after 24 h exposure to 90 μg ml^{-1} concentration of AuNP1-4, different in size and surface chemistry are shown in Fig. 2. Only hydrophilic, citrate-stabilized, 15 nm diameter AuNP3 were shown not to penetrate the SC into DSL.[33] Interestingly, surface modification of AuNP3 using thioglycolic acid and cetrimide, resulted in AuNP4 with hydrophobic surface showing skin penetration into deeper layers. A similar pattern was observed for the smaller particles, AuNP1 and AuNP2. Surface modification of hydrophobic AuNP1 using lecithin yielded hydrophilic AuNP2 with lower skin penetration ability under the experimental conditions, as indicated by the number of AuNP in the SC and DSL in representative optical z-stacks of the respective 10 μm thickness longitudinal skin sections examined by multiphoton microscopy (Fig. 3a). Therefore, nanoparticles with more hydrophobic character, AuNP1 and AuNP4, were more favorable for skin penetration. This indicates that nanoparticles, in this size range, follow the same penetration pathways postulated for the penetration of drug molecules. However their particulate nature will reduce the speed of diffusion[19] through the intercellular route dominated mainly by fluid lipidic pores.[41]

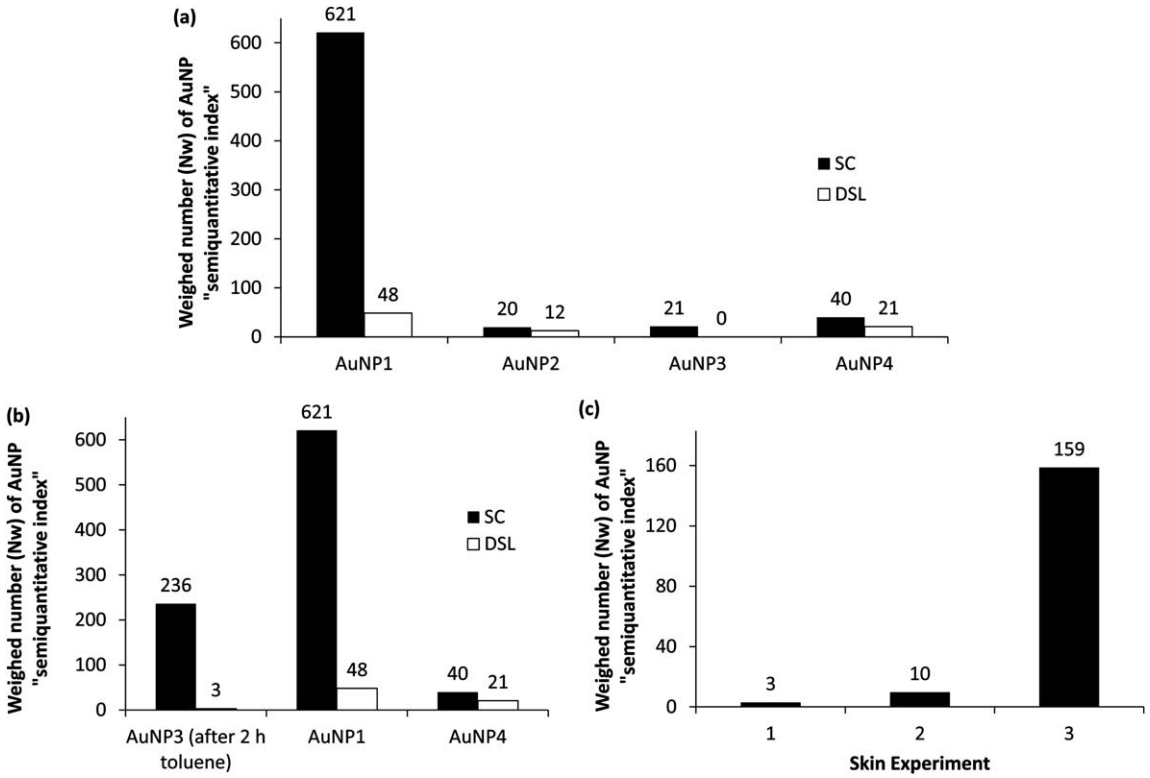

Fig. 3 The effect of the physicochemical parameters of nanoparticles, the vehicle and skin integrity on skin penetration of AuNP as extracted from optical layers of z-stacks (1 μm step width) of longitudinal skin sections imaged by multiphoton microscopy. (a) Skin penetration of AuNP1 (6 nm thiol-coated AuNP, dispersed in toluene), AuNP2 (6 nm lecithin-coated AuNP, dispersed in water), AuNP4 (15 nm cetrimide-coated AuNP, dispersed in toluene) at a concentration of 90 μg ml^{-1} of gold after 24 h of skin exposure. (b) Skin penetration of AuNP3 (15 nm citrate-stabilized AuNP, dispersed in water) on 22 h skin exposure following 2 h pre-exposure to toluene in comparison to skin penetration of AuNP1 and AuNP4 dispersed in toluene into the SC and DSL after 24 h of skin exposure. (c) Effect of 2 h pre-exposure to toluene "1" in comparison to removal of skin lipids using chloroform–methanol mixture, 2 : 1 "2" and to complete removal of the SC by tape stripping "3" on skin penetration of AuNP3 into DSL after 22 h of skin exposure.

Smaller sized AuNP1 and AuNP2, 6 nm in diameter, showed higher skin penetration than 15 nm AuNP3 (no penetration into DSL) and AuNP4, as shown in Fig. 3a. A similar pattern was also reported for drug penetration where high molecular weight compounds could penetrate the SC to a lesser extent than small molecules.[42] Though our results are partly contrary to the findings of Sonavane *et al.*[14] who showed skin permeation of AuNP, 15 nm in diameter after only 1 h (they used rat skin of different histology than human skin in our study), their results also indicated size-dependent skin permeation. According to them, higher permeation for 15 nm AuNP compared to 102 nm and 198 nm AuNP was indicated and the permeability coefficient was reported to decrease on increasing the particle size. Another report also indicated skin penetration of latex nanoparticles of 50, 100, 200 and 500 nm diameter in a size-dependent manner.[16]

Effect of the physical state of AuNP dispersion

The physical state of the applied nanodispersion, whether composed of individual particles or aggregated ones, is considered critical and should be analyzed carefully in parallel with the skin penetration study. This is to avoid any misinterpretation of the results in regard to the significance of particle size as a determinant of skin penetration. Here AuNP serve as a good model whose plasmon band provides precise and easily accessible information on the aggregation state of the colloidal gold. Aggregation is indicated by a large red-shift of the spectral peak and/or strong peak broadening.[43] Therefore, it was important to analyze the applied AuNP dispersion spectrophotometrically before and after the skin penetration experiment (Fig. 4). At the beginning of the skin experiment, all applied AuNP dispersions showed physical stability. No significant red-shift was observed for the test nanodispersions AuNP1, AuNP2 and AuNP4, applied at a concentration of 90 μg ml^{-1}, after 24 h of skin contact. However, after 24 h of skin exposure, aggregation was observed for AuNP3 (hydrophilic, citrate-stabilized and 15 nm in diameter) as evident from peak broadening (Fig. 4c). The zeta potential also increased by about 2-fold. Aggregation of AuNP3 could be attributed to the exchange of citrate ions on the surface of gold nanoparticles with skin proteins or lipids, as shown in other biological environments.[44,45] This could be also due to limited citrate ionization in the slightly acidic pH of the skin surface. This overnight aggregation further decreased the availability of single dispersed particles of higher probability to penetrate the SC into DSL (Fig. 2). On the other hand, all other particles (AuNP1, AuNP2 and AuNP4), penetrating the SC (Fig. 2), showed no significant aggregation following skin contact (Fig. 4a, b, d).

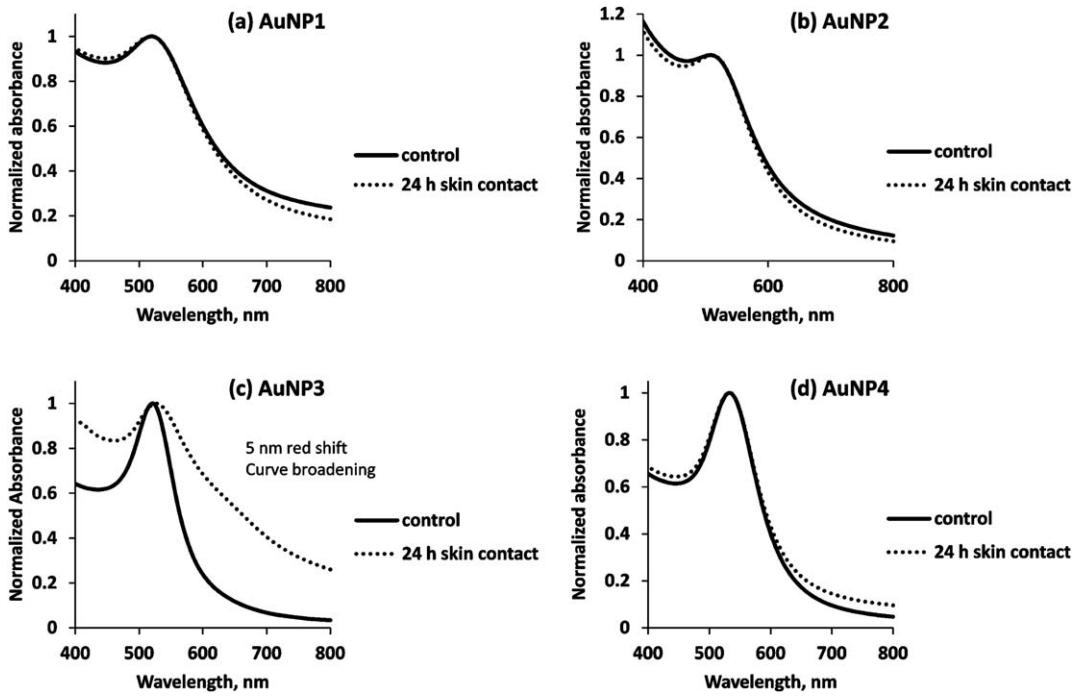

Fig. 4 UV/Vis spectra of (a) AuNP1 (6 nm thiol-coated AuNP, dispersed in toluene), (b) AuNP2 (6 nm lecithin-coated AuNP, dispersed in water), (c) AuNP3 (15 nm citrate-stabilized AuNP, dispersed in water) and (d) AuNP4 (15 nm cetrimide-coated AuNP, dispersed in toluene) at a concentration of 90 μg ml^{-1} of gold, showing particle stability before and after 24 h of skin contact.

Effect of the vehicle of AuNP dispersion

Beside the physicochemical properties of nanoparticles, the vehicle is known to influence skin penetration profiles. Hence this effect also should hold true for nanoparticle penetration. Unfortunately, this effect of the vehicle was usually disregarded in skin penetration studies of nanoparticles. Here, however, the effect of the vehicle was in the focus of this study. AuNP1 and AuNP4 were dispersed and applied in toluene, in comparison to AuNP2 and AuNP3 (water). Therefore, the effect of toluene under the applied experimental conditions on the intercellular lipids of the SC, providing the main barrier function,[41] was investigated. The percentages of lipid extracted from heat separated epidermal sheets on applying toluene for exposure times between 0.5–24 h, relative to the dry weight of the epidermis were determined by gravimetry (Table 3). These values were compared (as a percentage) to the total lipid content in the equivalent epidermal area for this skin donor (extracted by chloroform–methanol mixture, 2 : 1 after 24 h incubation), also calculated with respect to the dry weight of the epidermis. As shown in Table 3, a percentage of about 8–17% of the total epidermal lipid content was extracted by toluene. However, a closer look to the standard deviation values, one could conclude that the amount of lipid extracted by toluene is time-independent, *i.e.* the amount of lipid extracted after 0.5 h is not significantly different than that after 24 h.

Table 3 Gravimetric analysis of toluene lipid extract of heat separated epidermis after 0.5, 2, 6 and 24 h exposure time *versus* total epidermal lipids[a]

Incubation time/h	% lipid extracted with respect to dry skin wt	% lipid extracted with respect to total epidermal lipids
0.5	2.43 ± 0.08	7.82 ± 0.26
2	3.20 ± 1.25	10.29 ± 4.02
6	2.79 ± 1.89	8.97 ± 6.08
24	5.32 ± 3.29	17.08 ± 10.60
Control (total epidermal lipids)	31.13 ± 3.55	

[a] Determined by shaking epidermal sheets with chloroform/methanol mixture, 2 : 1 for 24 h.

Furthermore, the barrier function of the SC depends not only on the lipid quantity in the SC but also on the lipid composition. The main lipid classes in the SC are ceramides, cholesterol and fatty acids. Detection of triglycerides in the SC has been explained in the literature either by contamination with sebum glycerides or by extraction of subcutaneous fat. Other lipid ingredients present in minute amounts include cholesterol esters.[41,46] The quantitative composition of the SC lipids differs depending on the extraction method[47] and inter- and intra-individual variations. Among all the lipid members, ceramides are known to be the most important component of the SC multilamellar lipid structure with defined physicochemical properties necessary for the barrier function of the skin.[46] After 2 h of skin exposure, epidermal lipid members extracted by toluene or chloroform–methanol mixture (total lipid extract) were quantified using HPTLC *versus* increasing serial concentrations of standard lipid mixture. The lipid composition of each extract was then determined by densitometric analysis and the results are shown in Fig. 5. Toluene could extract the surface lipids; however, the structural lipids of the SC, ceramides, were not extracted by toluene. In contrast, ceramides were found in the total lipid extract of this skin donor.

Nevertheless, it could be concluded so far that toluene has an effect on the barrier function of the SC through lipid extraction. However, a drastic structural change in the skin barrier on toluene application is not likely, evident by the absence of ceramides in the toluene extract. Afterwards, it was important at this stage to determine whether the penetration of AuNP1 and AuNP4, dispersed in toluene, was mainly due to the effect of toluene on the barrier function of the skin, or this is only a contributing factor. Therefore, further skin penetration experiments were conducted, preincubating the skin with 500 μl toluene for 2 h, followed by application of non-penetrating AuNP3, dispersed in water. The number of AuNP penetrating into the SC and DSL in a representative z-stack of a 10 μm thickness skin section was semiquantified according to a method we published recently[20] and the result was compared to that due to application of AuNP1 and AuNP4, dispersed in toluene, at a concentration of 90 μg ml^{-1} for 24 h (Fig. 3b). It was found that the number of AuNP penetrating into DSL was 16- and 7-fold higher than that of AuNP1 and AuNP4, respectively. This indicates that penetration of nanoparticles did not depend mainly on the vehicle, toluene. Yet, it is a complex mechanism depending on several parameters; and removal of SC lipids enhances the penetration ability.

Effect of formulation ingredients

Skin penetration of nanoparticles should not be studied without considering formulation factors. Ingredients used in synthesis of nanoparticles could have an influence on their interaction with the skin when present in the dispersion. However, previous studies did not always take these factors into account when discussing nanoparticles penetration. This raises a question, whether nanoparticles do passively penetrate the SC due to their small size or this is a result of the physicochemical attributes of the nanoparticles as well as formulation, environmental and mechanical factors. In this study, chemicals used in particle synthesis could affect the skin hence possibly favoring more skin penetration including dodecanethiol and *tert*-butylamineborane (AuNP1), and thioglycolic acid (AuNP4). Furthermore, lecithin and cetrimide used in the preparation of AuNP2 and AuNP4, respectively are considered as penetration enhancers.[48] However, based on the amounts used relative to those described in literature,[48–50] they are assumed not to contribute much in skin penetration of nanoparticles. Yet, this is only an assumption and possibility for contribution is not discarded.

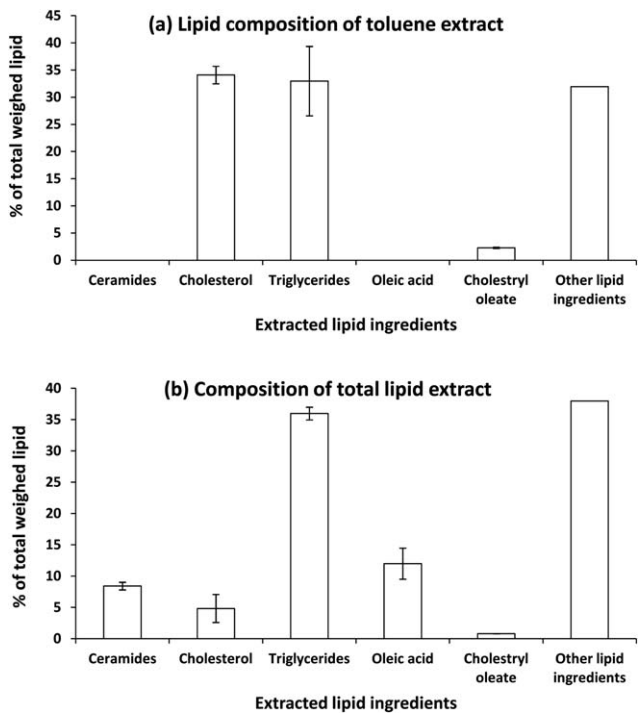

Fig. 5 Lipid composition of toluene extract of heat separated epidermis after 2 h of skin exposure time (a) *versus* total lipid extract using chloroform–methanol mixture, 2 : 1 (b).

Effect of deteriorating the barrier function of the SC

In general, damaged skin is assumed to facilitate penetration. Hence, additional experiments were carried out to determine the effect of deteriorating the skin barrier function (*i.e.*, the SC) on penetration of nanoparticles. AuNP3, shown not to penetrate into the DSL, were chosen for these experiments. The results were compared to skin penetration of AuNP3 after 2 h skin pre-exposure to toluene.

(1) Skin lipids were removed by treating the skin surface with 1 ml of chloroform–methanol mixture, 2 : 1 for 22 h. HPTLC of the applied mixture showed extraction of the epidermal lipids: ceramides, cholesterol, fatty acids (oleic acid), triglycerides and cholesteryl ester (cholesteryl oleate) (data not shown). Removal of epidermal lipids was then followed by application of AuNP3 for further 22 h. However, it should be noted here that in order to set up such an experiment a total of 44 h skin treatment was required (22 h for removal of epidermal lipids, followed by 22 h exposure to AuNP3). This would contribute to the penetrated amount due to decreased skin integrity.[51] Therefore, a supplementary experiment was performed which involves application of AuNP3 for only 2 h after skin treatment with a chloroform–methanol mixture for 22 h, *i.e.* a total of only 24 h skin experiment.

(2) The SC was completely removed by tape stripping 30-times followed by application of AuNP3 for 22 h. The experimental setup was carefully adjusted to insure that the stripped skin area is the same area exposed to nanoparticles. At the end of the penetration experiment, the skin surface was cleaned before further sectioning and examination by multiphoton microscopy.

As shown in Fig. 3c, removal of the skin lipids using chloroform–methanol mixture resulted in AuNP3 penetrating the SC after 22 h of skin exposure. Even on skin exposure to AuNP3 for 2 h (Data not shown), 2-fold increase in penetration into the DSL was observed, compared to skin penetration of AuNP3 after 2 h skin pre-exposure to toluene. This again confirms that as for drug molecules, the intercellular lipids are the main barrier for skin penetration of nanoparticles. Intercellular localization of nanoparticles was previously reported for QD.[52,53]

On the other hand, for tape-stripping, previous reports did not show satisfactory results concerning particle penetration on the tape stripping part of the SC for QD of diameter ~4 nm,[54] 6 nm[7] and ~37 nm[55] through human (20 tape-strips), rat (10 tape-strips) and mouse (5–20 tape-strips) skin, respectively. In this

study, complete removal of the SC by tape-stripping resulted, however, in about 16-fold further increase in penetration into DSL. This would rather indicate that the barrier function of the SC to particle penetration does not only rely on the intercellular lipids, however it is a complex mechanism that overall provides the rate-limiting step to penetration of nanoparticles.

For both conducted experiments, the number of AuNP3 penetrating into DSL was 2- and 53-fold, respectively, higher than that after 2 h exposure to toluene (Fig. 3c). This again supports our previously drawn conclusion that toluene does have an effect on skin penetration of AuNP, however it is only a contributing factor and not the main factor.

Effect of concentration of applied AuNP dispersion and skin exposure time

All studies investigating skin penetration of nanoparticles so far based their conclusion, whether the particles are penetrating or not on a single point concentration. This does not imply that their conclusion applies for dispersions with higher or lower concentrations leaving the reader sometimes with a degree of uncertainty about the results. This also partly explains the current controversy among researchers on the status of skin penetration of nanoparticles. Moreover, the duration of skin exposure to nanoparticles is very critical for studying the possible skin penetration of nanoparticles, since they diffuse slower. However, variable exposure times, *e.g.* 0.5,[56] 5,[3] 6,[15] 18[57] and 24[4] h, were reported in literature for *in vitro* particle penetration studies. Only few studies checked skin penetration on different time intervals. For instance, Baroli *et al.*[18] studied the penetration of magnetic nanoparticles through human skin after 3, 6, 12 and 24 h in which penetration was indicated by TEM images starting from 6 h skin exposure to the applied nanodispersion.

In this study, AuNP1 were applied on skin with two different concentrations, 90 and 437 μg ml^{-1} of gold, for exposure times of 0.5, 2, 6 and 24 h (Table 2). AuNP1 in both concentrations could penetrate the SC at 24 h. Applying AuNP1 dispersion with a concentration of 437 μg ml^{-1} resulted in higher number of AuNP in z-sections of longitudinal skin sections of 10 μm thickness in the SC as well as in DSL (Fig. 6). For the two tested

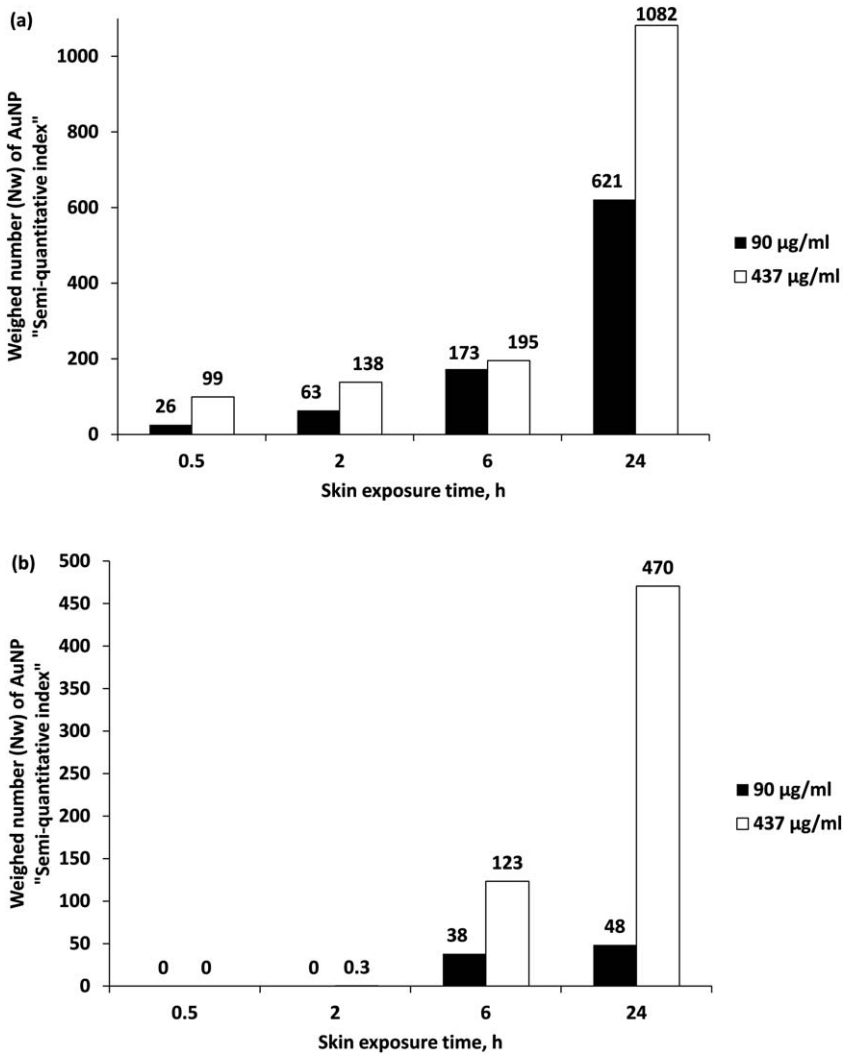

Fig. 6 Effect of concentration of applied AuNP1 (6 nm thiol-coated AuNP, dispersed in toluene) and skin exposure time on their penetration into the SC (a) and DSL (b) after 24 h of skin exposure.

Table 4 Maximum skin penetration depths of AuNP1 (6 nm thiol-coated AuNP, dispersed in toluene) in 90 and 437 μg ml^{-1} concentration after 0.5, 2, 6 and 24 h of skin exposure, normalized to the thickness of the SC (i) and penetration depth inside DSL after crossing the whole thickness of SC (ii)

(i)

	[a]Percentage depth of SC penetrated by AuNP1 [%]	
Incubation time/h	90 μg ml^{-1}	437 μg ml^{-1}
0.5	48.55	77.99
2	92.65	100
6	100	100
24	100	100

(ii)

	[b]Penetration depth of AuNP1 in DSL/μm	
Incubation time/h	90 μg ml^{-1}	437 μg ml^{-1}
0.5	0	0
2	0	23.86
6	7.21	29.82
24	35.72	51.38

[a] Percentage SC penetrated= penetration depth in SC/thickness of SC × 100. [b] Penetration depth in DSL = Total penetration depth - thickness of SC.

concentrations, the incubation time showed a strong effect on the amount of AuNP penetrating into the SC and DSL. An exposure time of 6 h was required for AuNP1 with a concentration of 90 μg ml^{-1} to permeate the SC whereas 2 h were enough for the high concentration AuNP dispersion (437 μg ml^{-1}) to penetrate into the DSL though this was a negligible amount. The longer the skin exposure time, the larger the amount of AuNP1 penetrating into the SC and DSL (Fig. 6). This is also attributed to the amount of particles necessary for detection, favoring high concentrations to be visualized.

Maximum penetration depths of AuNP1 inside the skin were further determined for these skin penetration experiments (Table 4). The same trend was also observed on changing the concentration and the skin exposure time. The higher the concentration and/or the longer the skin exposure time, the longer the distance that could be travelled by AuNP1 inside the skin. The longest penetration depth by AuNP1 in DSL after crossing the whole thickness of the SC was 51.38 μm (Table 4). Knowing that the average thickness of the viable epidermis is 50–100 μm,[58] particles could only reach the viable epidermis of human skin after 24 h of skin exposure. Longer exposure times could be needed for the particles to penetrate further into the dermis, however skin penetration experiments were terminated at 24 h to avoid loss of skin integrity.[51]

On further analysis of Fig. 6, one could observe a gradually increasing difference between the density of particle localization in the DSL for the two applied concentrations with time, reaching a maximum at 24 h. This could be attributed to:

(a) The higher the concentration of the nanodispersion the more particles are available for penetration, leading to much more particle accumulation in the deeper skin layers.

(b) The higher concentration dispersion requires also a shorter exposure time (2 h) than that at low concentration (6 h) to cross the stratum corneum (Table 4), leading to a higher cumulative concentration of particles in the deeper skin layer.

It should be noted here that the whole area of the deeper skin layer in the image field is included in the analysis. This means that the concentration measured is a more-or-less "cumulative" concentration.

Based on this, care should be taken on meta-analysis of the available literature on skin nanoparticle penetration. This means that extrapolation of the studies based on a single concentration or a short exposure time to indicate safety of nanoparticles or the opposite case should be avoided.

Conclusions

As is the case for drug molecules, the main barrier for particle penetration is the SC, however it is not only the intercellular lipids that limit penetration of particles but the whole microstructure of the SC with its tortuous intercellular aqueous and lipidic channels. Furthermore, the varying polarities of the skin layers further reduce permeation into deeper skin layers. AuNP are expected to penetrate mainly through intercellular pathways. This penetration behavior is primarily dependent on their physicochemical attributes, of which the size is the most significant determinant of penetration where 6 nm AuNP showed a greater extent of penetration than 15 nm AuNP. Similar to drug penetration, the surface hydrophobicity was also found as an important factor favoring skin penetration. This again implies that nanoparticles at this size range (6–15 nm) behave similar to drug molecules in permeation through the skin barrier, but to a lower extent. On the other hand, the vehicle was found to have a minimal effect on skin penetration of AuNP.

Skin exposure time was also found to be of crucial impact. Incubation times of at least 6 h were required to have a significant penetration extent for studying the effect of the different physicochemical, formulation and environmental factors. Shorter exposure times are thus not recommended by the authors for conducting experiments focusing on determination of skin penetration of nanoparticles. For a certain skin exposure time, the concentration of the applied nanodispersion could greatly influence or even determine the status of skin penetration of nanoparticles, whether they could be detected or not in the DSL. This should be regarded in future studies. The results obtained in this study are of great importance, especially for the basic understanding of the interaction of nanoparticles with the skin barrier.

Acknowledgements

This work was supported by the Ministry of Higher Education and Scientific Research, Egypt "MHESR" and Deutscher Akademischer Austausch Dienst "DAAD". Thanks to Leon Muijs for preparing the longitudinal skin sections; Peter Meiers for his help with HPTLC; Tsambika Hahn for the fruitful discussions and help; and Christian Cavelius for his help in transferring

apolar gold nanoparticles into the aqueous phase. TEM images have been realized by Nico Reum.

References

1 J. P. Ryman-Rasmussen, J. E. Riviere and N. A. Monteiro-Riviere, *Toxicol. Sci.*, 2006, **91**, 159–165.
2 S. H. Jeong, J. H. Kim, S. M. Yi, J. P. Lee, J. H. Kim, K. H. Sohn, K. L. Park, M.-K. Kim and S. W. Son, *Biochem. Biophys. Res. Commun.*, 2010, **394**, 612–615.
3 F. Stracke, B. Weiss, C. M. Lehr, K. Konig, U. F. Schaefer and M. Schneider, *J. Invest. Dermatol.*, 2006, **126**, 2224–2233.
4 S. E. Cross, B. Innes, M. S. Roberts, T. Tsuzuki, T. A. Robertson and P. McCormick, *Skin Pharmacol. Physiol.*, 2007, **20**, 148–154.
5 P. Filipe, J. N. Silva, R. Silva, J. L. Cirne de Castro, M. Marques Gomes, L. C. Alves, R. Santus and T. Pinheiro, *Skin Pharmacol. Physiol.*, 2009, **22**, 266–275.
6 T. W. Prow, N. A. Monteiro-Riviere, A. O. Inman, J. E. Grice, X. Chen, X. Zhao, W. H. Sanchez, A. Gierden, M. A. Kendall, A. V. Zvyagin, D. Erdmann, J. E. Riviere and M. S. Roberts, *Nanotoxicology*, 2011.
7 L. W. Zhang and N. A. Monteiro-Riviere, *Skin Pharmacol. Physiol.*, 2008, **21**, 166–180.
8 J. G. Rouse, J. Yang, J. P. Ryman-Rasmussen, A. R. Barron and N. A. Monteiro-Riviere, *Nano Lett.*, 2007, **7**, 155–160.
9 L. J. Mortensen, G. Oberdorster, A. P. Pentland and L. A. Delouise, *Nano Lett.*, 2008, **8**, 2779–2787.
10 S. Paliwal, G. K. Menon and S. Mitragotri, *J. Invest. Dermatol.*, 2006, **126**, 1095–1101.
11 S. A. Coulman, A. Anstey, C. Gateley, A. Morrissey, P. McLoughlin, C. Allender and J. C. Birchall, *Int. J. Pharm.*, 2009, **366**, 190–200.
12 T. R. Kuo, C. L. Wu, C. T. Hsu, W. Lo, S. J. Chiang, S. J. Lin, C. Y. Dong and C. C. Chen, *Biomaterials*, 2009, **30**, 3002–3008.
13 X. R. Xia, N. A. Monteiro-Riviere and J. E. Riviere, *Toxicol. Appl. Pharmacol.*, 2010, **242**, 29–37.
14 G. Sonavane, K. Tomoda, A. Sano, H. Ohshima, H. Terada and K. Makino, *Colloids Surf., B*, 2008, **65**, 1–10.
15 X. Wu, K. Landfester, A. Musyanovych and R. H. Guy, *Skin Pharmacol. Physiol.*, 2010, **23**, 117–123.
16 A. K. Kohli and H. O. Alpar, *Int. J. Pharm.*, 2004, **275**, 13–17.
17 M. Senzui, T. Tamura, K. Miura, Y. Ikarashi, Y. Watanabe and M. Fujii, *J. Toxicol. Sci.*, 2010, **35**, 107–113.
18 B. Baroli, M. G. Ennas, F. Loffredo, M. Isola, R. Pinna and M. A. Lopez-Quintela, *J. Invest. Dermatol.*, 2007, **127**, 1701–1712.
19 M. Schneider, F. Stracke, S. Hansen and U. F. Schaefer, *Derm.-Endocrinol.*, 2009, **1**, 197–206.
20 H. I. Labouta, T. Kraus, L. K. El-Khordagui and M. Schneider, *Int. J. Pharm.*, 2011, **413**, 279–282.
21 F. Larese Filon, M. Crosera, G. Adami, M. Bovenzi, F. Rossi and G. Maina, *Nanotoxicology*, 2011.
22 Y. Huang, F. Yu, Y. S. Park, J. Wang, M. C. Shin, H. S. Chung and V. C. Yang, *Biomaterials*, 2010, **31**, 9086–9091.
23 G. Schmid, *Chem. Rev.*, 1992, **92**, 1709–1727.
24 P. Ghosh, G. Han, M. De, C. K. Kim and V. M. Rotello, *Adv. Drug Delivery Rev.*, 2008, **60**, 1307–1315.
25 H. I. Labouta and M. Schneider, *Int. J. Pharm.*, 2010, **395**, 236–242.
26 D. Pissuwan, T. Niidome and M. B. Cortie, *J. Controlled Release*, 2011, **149**, 65–71.
27 N. Reum, C. Fink-Straube, T. Klein, R. W. Hartmann, C. M. Lehr and M. Schneider, *Langmuir*, 2010, **26**, 16901–16908.
28 D. Bhumkar, H. Joshi, M. Sastry and V. Pokharkar, *Pharm. Res.*, 2007, **24**, 1415–1426.
29 H. Wang, H. Huang and X. Huang, *Plant Growth Regul.*, 2007, **52**, 189–198.
30 M. Thomas and A. M. Klibanov, *Proc. Natl. Acad. Sci. U. S. A.*, 2003, **100**, 9138–9143.
31 M. Oishi, J. Nakaogami, T. Ishii and Y. Nagasaki, *Chem. Lett.*, 2006, **35**, 1046–1047.
32 X. Huang, W. Qian, I. H. El-Sayed and M. A. El-Sayed, *Lasers Surg. Med.*, 2007, **39**, 747–753.
33 H. I. Labouta, D. C. Liu, L. L. Lin, M. K. Butler, G. E. Jeffrey, A. Raphael, T. Kraus, L. K. El-Khordagui, H. P. Soyer, M. S. Roberts, M. Schneider and T. W. Prow, *Pharm. Res.*, 2011, **28**, 2931, DOI: 10.1007/s11095-011-0561-z.
34 N. Zheng, J. Fan and G. D. Stucky, *J. Am. Chem. Soc.*, 2006, **128**, 6550–6551.
35 J. Turkevich, P. C. Stevenson and J. Hillier, *Discuss. Faraday Soc.*, 1951, **11**, 55–57.
36 H. Zhu, C. Tao, S. Zheng, S. Wu and J. Li, *Colloids Surf., A*, 2005, **256**, 17–20.
37 H. Wagner, K. H. Kostka, W. Adelhardt and U. F. Schaefer, *Eur. J. Pharm. Biopharm.*, 2004, **58**, 121–129.
38 T. Hahn, S. Hansen, D. Neumann, K. H. Kostka, C. M. Lehr, L. Muys and U. F. Schaefer, *Skin Pharmacol. Physiol.*, 2010, **23**, 183–192.
39 A. M. Kligman and E. Christophers, *Arch. Dermatol.*, 1963, **88**, 702–705.
40 H. I. Labouta, M. Hampel, S. Thude, K. Reutlinger, K. H. Kostka and M. Schneider, *J. Biophotonics*, 2011, DOI: 10.1002/jbio.201100069, in press.
41 P. W. Wertz, *Acta Derm.-Venereol.*, 2000, **80**, 7–11.
42 B. M. Magnusson, Y. G. Anissimov, S. E. Cross and M. S. Roberts, *J. Invest. Dermatol.*, 2004, **122**, 993–999.
43 G. Schneider and G. Decher, *Langmuir*, 2008, **24**, 1778–1789.
44 A. S. Parfenov, V. Salnikov, W. J. Lederer and V. Lukyánenko, *Biophys. J.*, 2006, **90**, 1107–1119.
45 S. H. Lacerda, J. J. Park, C. Meuse, D. Pristinski, M. L. Becker, A. Karim and J. F. Douglas, *ACS Nano*, 2010, **4**, 365–379.
46 B. Glombitza and C. C. Müller-Goymann, *Chem. Phys. Lipids*, 2002, **117**, 29–44.
47 N. A. Monteiro-Riviere, A. O. Inman, V. Mak, P. Wertz and J. E. Riviere, *Pharm. Res.*, 2001, **18**, 992–998.
48 H. Y. Thong, H. Zhai and H. I. Maibach, *Skin Pharmacol. Physiol.*, 2007, **20**, 272–282.
49 H. K. Vaddi, L. Z. Wang, P. C. Ho and S. Y. Chan, *Int. J. Pharm.*, 2001, **212**, 247–255.
50 H. Zhou, Y. Yue, G. Liu, Y. Li, J. Zhang, Q. Gong, Z. Yan and M. Duan, *Nanoscale Res. Lett.*, 2009, **5**, 224–230.
51 OECD, in *OECD Guideline for the Testing of Chemicals*, 23 November 2004.
52 L. W. Zhang, W. W. Yu, V. L. Colvin and N. A. Monteiro-Riviere, *Toxicol. Appl. Pharmacol.*, 2008, **228**, 200–211.
53 P. Upadhyay, *Vaccine*, 2006, **24**, 5593–5598.
54 T. Gratieri, U. F. Schaefer, L. Jing, M. Gao, R. F. V. Lopez and M. Schneider, *J. Biomed. Nanotechnol.*, 2010, **6**, 586–595.
55 N. V. Gopee, D. W. Roberts, P. Webb, C. R. Cozart, P. H. Siitonen, J. R. Latendresse, A. R. Warbitton, W. W. Yu, V. L. Colvin, N. J. Walker and P. C. Howard, *Toxicol. Sci.*, 2009, **111**, 37–48.
56 J. Luengo, B. Weiss, M. Schneider, A. Ehlers, F. Stracke, K. Konig, K. H. Kostka, C. M. Lehr and U. F. Schaefer, *Skin Pharmacol. Physiol.*, 2006, **19**, 190–197.
57 J. Shim, H. Seok Kang, W. S. Park, S. H. Han, J. Kim and I. S. Chang, *J. Controlled Release*, 2004, **97**, 477–484.
58 G. Cevc, *Adv. Drug Delivery Rev.*, 2004, **56**, 675–711.